Molecular Biology of the Cell
Vol. 7, 1749–1758, November 1996

Spatial Organization of the Nim1-Wee1-Cdc2 Mitotic Control Network in *Schizosaccharomyces pombe*

Lin Wu, Kazuhiro Shiozaki, Rosa Aligue,* and Paul Russell†

Departments of Molecular Biology and Cell Biology, The Scripps Research Institute, La Jolla, California 92037

Submitted June 4, 1996; Accepted August 14, 1996
Monitoring Editor: Mitsuhiro Yanagida

In *Schizosaccharomyces pombe* the onset of mitosis is regulated by a network of protein kinases and phosphatases. The M-phase inducing Cdc2-Cdc13 cyclin-dependent kinase is inhibited by Wee1 tyrosine kinase and activated by Cdc25 phosphatase. Wee1 is negatively regulated by Nim1 protein kinase. Here, we describe investigations aimed at better understanding the role of Nim1 in the mitotic control. The most important finding to emerge from these studies is that Wee1 and Nim1 have different patterns of intracellular localization. Immunofluorescence confocal microscopy has revealed that Nim1 is localized in the cytoplasm, whereas its substrate Wee1 is predominantly localized in the nucleus. Previous studies showed that the Cdc2-Cdc13 complex is located in the nucleus. Diversion of Nim1 to the nucleus, accomplished by addition of the SV40 nuclear localization signal, caused the advancement of M, confirming that Nim1 has restricted access to Wee1 in vivo. We propose that the intracellular distribution of Nim1 and Wee1 may serve to coordinate the regulation of nuclear Cdc2-Cdc13 with cytoplasmic growth.

INTRODUCTION

The molecular mechanisms regulating the onset of mitosis have been intensively studied in the fission yeast *Schizosaccharomyces pombe*. The initiation of mitosis is brought about by a cyclin-dependent kinase consisting of a catalytic subunit encoded by *cdc2*$^+$ and a B-type cyclin encoded by *cdc13*$^+$ (Booher *et al.*, 1989; Moreno *et al.*, 1989). Cdc13 accumulates during interphase and associates with Cdc2. Activity of this complex requires phosphorylation of the threonine-167 residue of Cdc2 (Gould *et al.*, 1991). In contrast to the positive effect of threonine-167 phosphorylation, phosphorylation on tyrosine-15 inhibits Cdc2 activity (Gould and Nurse, 1989). This phosphorylation is performed by Wee1 and Mik1 tyrosine kinases, with Wee1 having the dominant role (Nurse, 1975; Russell and Nurse, 1987b; Featherstone and Russell, 1991; Lundgren *et al.*, 1991; Parker *et al.*, 1992; McGowan and Russell, 1993; Lee *et al.*, 1994). Simultaneous inactivation of Wee1 and Mik1 results in a mitotic catastrophe phenotype due to premature induction of mitosis (Lundgren *et al.*, 1991). Cdc2-Cdc13 kinase is activated by Tyr−15 dephosphorylation carried out by Cdc25 and Pyp3 protein tyrosine phosphatases, with Cdc25 having the dominant role (Russell and Nurse, 1986; Gould and Nurse, 1989; Gould *et al.*, 1990; Millar *et al.*, 1991–1992; Kovelman and Russell, 1996).

The protein kinases and phosphatases that regulate Cdc2-Cdc13 are themselves regulated by phosphorylation (Dunphy, 1994). Genetic studies first suggested that Wee1 is inhibited by Nim1/Cdr1 protein kinase. The *nim1*$^+$ gene was initially cloned as a multicopy suppressor of the *cdc25-22* temperature-sensitive mutation (Russell and Nurse, 1987a). The *nim1*$^+$ gene was later shown to be allelic to *cdr1*$^+$ (Young and Fantes, 1987; Feilotter *et al.*, 1991). Disruption of *nim1*$^+$ delays mitosis, causing cells to grow to a larger cell size before initiating mitosis. Conversely, overexpression of *nim1*$^+$ advances the onset of mitosis, causing cells to divide at a reduced cell size. Nim1 overproduction is lethal in a *mik1*$^-$ background but not in a *wee1*$^-$ background, which suggested that Nim1 specifically caused the inhibition of Wee1 activity (Wu and Russell, 1993). Metabolic labeling experiments showed that Nim1 promoted Wee1 phosphorylation in vivo

* Present address: Department of Cell Biology, Faculty of Medicine, University of Barcelona, Barcelona, Spain.
† Corresponding author.

(Wu and Russell, 1993). These findings were confirmed by in vitro studies which showed that Nim1 inhibited Wee1 activity by direct phosphorylation of the catalytic domain of Wee1 (Coleman *et al.*, 1993; Parker *et al.*, 1993; Wu and Russell, 1993).

Although it is clearly established that Nim1 functions as a mitotic inducer by inhibiting Wee1, the regulation of Nim1 in the mitotic control is uncertain. *cdr1*$^-$ mutations were isolated in a visual screen of mutants that failed to become small when starved of nitrogen, suggesting that Nim1 (Cdr1) may have a special role in coordinating the mitotic control with nutrient availability (Young and Fantes, 1987). However, *nim1*$^-$ mutants are also elongated when grown in rich nutrient medium, suggesting that Nim1 has an important role in inducing mitosis in all growth conditions (Russell and Nurse, 1987a). Moreover, *nim1*$^-$ mutants have no reported defects in mating or survival when starved of nitrogen, thus it is unclear whether Nim1 has a special role in regulating mitosis in response to nutrient limitation. With the goal of understanding the role of Nim1 in the mitotic control, we have undertaken an investigation of the temporal and spatial expression of Nim1 protein during the mitotic cell cycle. A key finding to emerge from these studies is that Nim1 is predominantly localized in the cytoplasm whereas its substrate, Wee1, is predominantly localized in the nucleus along with its substrate Cdc2-Cdc13. These studies suggest that Nim1 may have an important role in linking the regulation of nuclear Cdc2-Cdc13 kinase with the cytoplasm.

MATERIALS AND METHODS

Yeast Strains and Media

Schizosaccharomyces pombe strains constructed for this study are listed in Table 1. They are all derived from *972h*$^-$ and *975h*$^+$ (Mitchison, 1970). Procedures for genetic studies in *S. pombe* have been described (Moreno *et al.*, 1991). YES and synthetic EMM2 media were used to grow *S. pombe* cells (Moreno *et al.*, 1991). Cell size measurements were determined using an eyepiece micrometer attached to a Zeiss Axioskop 20 microscope with a 100× objective; at least 20 cells from each strain were measured.

Chromosomal Integration of nim1-Ha6H

The *Sph*I/*Eco*RI fragment from plasmid pREP1-Nim1 (Wu and Russell, 1993) was ligated into pUR19^{ars-}. pUR19^{ars-} was created by removing the *Cla*I fragment containing ars1 from pUR19 (Barbet *et al.*, 1992). The resulting plasmid pUR19^{ars-} Nim1 contains promoterless *nim1*$^+$, which also lacks the first 90 bp of its open reading frame. A sequence encoding two copies of the HA epitope tag and six consecutive histidines was inserted just before the stop codon (Wu and Russell, 1993). Plasmid pUR19^{ars-}Nim1-Ha6H was digested at the single *Xho*I site in the *nim1*$^+$ open reading frame and then integrated via homologous recombination into the *nim1*$^+$ locus of a *leu1-32 ura4-D18* strain. Stable Ura$^+$ transformants were selected and confirmed by Southern blot hybridization. The expression of Nim1-Ha6H was confirmed by immunoblot analysis.

Table 1. *S. pombe* strains used in this study

Strain	Genotype	Reference
PR109	*h*$^-$	PR stock
PR181	*h*$^+$ *cdc2-33*	PR stock
PR196	*h*$^+$ *cdc25-22*	PR stock
PR369	*h*$^-$ *adh1:nim1*$^+$ *adh1:wee1-50*	Wu and Russell, 1993
LW110	*h*$^-$ *nim1-Ha6H cdc10-129*	This study
LW117	*h*$^-$ *nim1-Ha6H*	This study
LW232	*h*$^-$ *nim1-Ha6H cdc25-22*	This study
LW388	*h*$^-$ *nim1::ura4*$^+$	This study
PR387	*h*$^-$ *nim1::LEU2*	Russell and Nurse, 1987a
LW424	*h*$^-$ *nim1-NLS*	This study
LW425	*h*$^-$ *nim1-NLS**	This study
LW449	*h*$^-$ *pLW182*-multiple integrant of *nim1*$^+$	This study

All strains were *leu1-32 ura4-D18*.

Multiple Integration of nim1$^+$

The C-terminal and 3′ untranslated sequence of *nim1*$^+$ was PCR amplified from *S. pombe* genomic DNA using these primers: 5′-GGG CGC GAT GAT ATG TTG AAA-3′ and 5′-GGG TCG ACA GAG GTA AAC GGT TTA TAG GAA-3′. The PCR product was digested with *Hin*dIII and *Sal*I and ligated into pUR19^{ars-}, creating plasmid pLW180. The 6-kb *Hin*dIII fragment from pNim1-12 (Russell and Nurse, 1987a) was ligated into the *Hin*dIII site of pLW180 to create plasmid pLW182, which contains the full-length *nim1*$^+$ open reading frame with 5′ and 3′ flanking sequences. A *leu1-32 ura4-D18* strain was transformed with the *Xho*I-digested product of pLW182. Stable Ura$^+$ transformants were selected and the expression level of Nim1 protein was compared with wild-type cells by immunoblot analysis using affinity-purified anti-Nim1 9805 antibody (Wu and Russell, 1993).

Chromosomal Replacement of nim1$^+$ by nim1-nls or nim1-nls*

The *Xho*I/*Not*I fragment of pREP1-Nim1 (Wu and Russell, 1993) was cloned into pBluescript, generating pLW145. The 1.8-kb *Hin*dIII fragment containing *ura4*$^+$ was inserted into the *Hin*dIII site of pLW145 to generate pLW146. The *Xho*I/*Bgl*II fragment of this plasmid was transformed into a *leu1-32 ura4-D18* strain. Stable Ura4$^+$ transformants were selected and confirmed by Southern blot hybridization. The resulting *nim1::ura4*$^+$ strain was named LW388. Sequences encoding the wild-type SV40 NLS (PKKKRKV) or the mutant NLS* (PKNKRKV) were inserted just before the *nim1*$^+$ termination codon by PCR. The sequence of the 5′ primer for nim1-nls was 5′-GGG CGG CCG CCC TAA GAA GAA GCG TAA GGT CGA CTA AAT AGG AAT TTT TTC AAA AAC A-3′. The 5′ primer for nim1-nls* was 5′-GGG CGG CCG CCC TAA GAA TAA GCG TAA GGT CGA CTA AAT AGG AAT TTT TTC AAA AAC A-3′. The 3′ primer for both PCR reactions was GGA CTA GTG TGC CCA AAT CAT T-3′. The PCR products were cloned into PCRII, generating plasmids pLW160 and pLW162, respectively. The *Not*I/*Sst*I fragments from pLW160 and pLW162 were cloned into pLW145 partially digested by *Not*I and *Sst*I to generate pLW170 and pLW171, respectively. The *Xho*I/*Spe*I fragment of pLW170 or pLW171 was cotransformed into strain LW388 with the reporter plasmid pART1. Leu$^+$ transformants were replica printed onto 5′ FOA plates to select against Ura4$^+$ cells. The 5′ FOA-resistant colonies were further analyzed by Southern blot hybridization to confirm the correct replacement of *nim1*$^+$ with *nim1-nls* or *nim1-nls**.

Immunoblotting of Nim1-Ha6H

Approximately 20 A_{600} of *S. pombe* cells from each time point were lysed in 0.550 ml of Denature buffer (6 M guanidine hydrochloride, 0.1 M sodium phosphate, 20 mM Tris, pH 8.0) in a 1.5-ml microfuge tube. After adding glass beads to the meniscus, cells were vigorously vortexed and the supernatant was collected after a high-speed spin (14,000 × *g* for 10 min). The protein concentration was measured with the Bradford assay and an equal amount of protein was added to Ni^{2+}-NTA beads washed according to the manufacturer's instruction (QIAGEN, Chatsworth, CA). Samples were washed as described (Shiozaki and Russell, 1995). Sequential precipitations confirmed that essentially 100% of the Nim1-Ha6H protein is purified in the first round of Ni^{2+}-NTA absorption. The bound protein was analyzed by immunoblotting using anti-Nim1 sera (antibody 9805). Membranes were stained with Ponceau S to confirm that equal amounts of a ~50-kDa protein that specifically binds to Ni^{2+}-NTA were present in each lane.

Phosphatase Treatment of Nim1

Two units of potato acid phosphatase (Boehringer Mannheim, Indianapolis, IN) were dissolved into 0.20 ml of phosphatase buffer (0.1 M Mes(2-[N-Morpholino]ethane-sulfonic acid), pH 6.0, 1 mM dithiothreitol) in the presence of protease inhibitors (1 μg/ml each of leupeptin, aprotinin, and pepstatin and 1 mM phenylmethylsulfonyl fluoride). The mixture was then added to immobilized protein samples and incubated at 30°C for 30 min.

Immunoblotting of Nim1 from Whole Cell Extracts

Approximately 20 A_{600} of cells were lysed in 0.2 ml of lysis buffer (50 mM Tris, pH 8.0, 150 mM NaCl, 10 mM EDTA, 10% glycerol, 50 mM NaF, 1 μg/ml each of leupeptin, aprotinin, and pepstatin, 1 mM PMSF, 1 mM dithiothreitol) in a 1.5-ml microfuge tube. Glass beads were added to the samples and the tubes were vortexed vigorously in the cold room for 5 min. Cell extracts were mixed 1:1 in SDS sample loading buffer. These samples were then boiled at 100°C for 2 to 3 min. After centrifugation (10,000 × *g* for 5 min), the protein concentration in the supernatant was estimated by measuring A_{280}. Equal amounts of protein were loaded from each sample. The proteins were separated on 8 to 15% SDS-polyacrylamide gradient gels and analyzed by immunoblotting using affinity-purified anti-Nim1 antibody 9805.

Confocal Immunofluorescence Microscopy

Fixative solution was made by dissolving 6 g of paraformaldehyde in 20 ml of PEM buffer (100 mM piperazine-*N*,*N*′-bis(2-ethanesulfonic acid), 1 mM EGTA, 1 mM $MgSO_4$, pH 6.9). The mixture was incubated at 65°C for 30 min. NaOH was added to dissolve most of the paraformaldehyde. This solution was diluted 1/10 into a growing culture to fix cells. After a 1-h incubation, cells were collected and washed in PEM. Cells were then resuspended in PEMS (PEM + 1 M sorbitol) with 0.625 mg/ml Zymolyase-20T (20,000 U/g; Seikagaku America, Rockville, MD) and 0.1 mg/ml NovoZym (Novo Industrials, Bagsvaerd, Denmark) and incubated for 0.5 to 1 h at 37°C. Cells were collected and resuspended in PEMS + 1% Triton X-100 for 1 min. They were washed three times with PEM and incubated in PEMBAL (PEM supplemented with 1% bovine serum albumin, 0.1% sodium azide, 100 mM L-lysine monohydrochloride, pH 6.9) for 1 h at room temperature. Affinity-purified anti-Nim1 (antibody 9805) or anti-Wee1 (antibody 7451) antibodies were added in PEMBAL, and the samples were incubated overnight at room temperature. After washing three times with PEMBAL, cells were incubated for 1 h at room temperature in PEMBAL containing fluorescein isothiocyanate (FITC)-conjugated goat anti-rabbit IgG antibody (1/50 dilution) and RNase A (200 μg/ml). After the final wash with PEMBAL, samples were resuspended in PBS containing 0.1% sodium azide and 4 μg/ml propidium iodide. SlowFade Antifade kit (Molecular Probes, Eugene, OR) was used for mounting. Cells were examined using a Bio-Rad MRC 600 confocal laser scanning microscope. The FITC (anti-Wee1 or anti-Nim1) and propidium iodide signals were merged using Adobe Photoshop software.

RESULTS

Cell Cycle Regulation of Nim1 mRNA and Protein Abundance

The aim of our investigations was to characterize the temporal and spatial patterns of Nim1 mRNA and protein expression during the mitotic cell cycle. We first carried out an experiment to measure the abundance of *nim1*$^+$ mRNA. Cells were synchronized by a *cdc25-22* arrest and release protocol, which temporarily blocks cells in G_2 and then synchronously releases them into the M phase (Figure 1). In this experiment the *nim1*$^+$ and the *adh1*$^+$ control mRNA signals remained approximately constant during the ensuing cell cycles. Cell cycle periodicity was confirmed by the dramatic oscillation of the *cdc22*$^+$ mRNA signal (Figure 1), which appears during the S phase (Lowndes *et al.*, 1992).

We next determined whether the abundance of Nim1 protein changed during the cell cycle. The extreme paucity of Nim1 protein in wild-type cells made it very difficult to detect Nim1 by immunoblotting of whole cell lysates, and this was true even for a strain that expressed a wild-type level of Nim1 containing three copies of the HA epitope (our unpublished

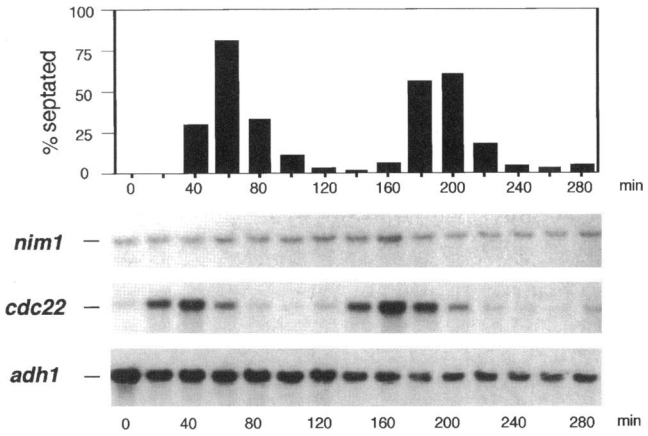

Figure 1. The abundance of *nim1*$^+$ mRNA does not oscillate during the cell cycle. A *cdc25-22* strain (PR196) was grown at 25°C in YES media to early log phase, and cells were arrested in G_2 by incubating at 36°C for 4 h and synchronously released into the cell cycle by reducing the culture temperature to 25°C. Samples were taken every 20 min. Cell cycle progression was monitored by determining the septation index (top panel). Total RNA was extracted and Northern blot hybridization was performed using probes for *nim1*$^+$, *cdc22*$^+$, and *adh1*$^+$. The latter two probes served as controls: *cdc22*$^+$ mRNA appears periodically during the S phase, whereas the amount of *adh1*$^+$ mRNA is constant during the cell cycle.

data). The Nim1 detection problem was easily solved by constructing a strain in which the genomic copy of *nim1*$^+$ was replaced with a copy of *nim1*$^+$ that encoded Nim1 protein having a C-terminal tag consisting of two copies of the HA epitope followed by six consecutive histidine residues (Wu and Russell, 1993). This strain divided at a cell length similar to that of the wild type, indicating that the epitope tag did not impair Nim1 activity. The His tag allowed efficient purification of Nim1 using Ni^{2+}-NTA chromatography matrix in denaturing conditions. A similar approach has been used to study Spc1 kinase in *S. pombe* (Shiozaki and Russell, 1995). The method used to normalize samples is described in Materials and Methods. A synchronized population of small cells in early G_2 was produced by centrifugal elutriation. Samples were taken at regular intervals for two cell cycles and then processed for Nim1 purification and immunoblotting. As previously noted (Wu and Russell, 1993), Nim1 protein was detected as a rather broad series of bands in the ~70- kDa region of the gel (Figure 2A). The appearance of the slower mobility species of Nim1 was attributed to an autophosphorylation activity (Fig. 2, B and C) because they were lost following in vitro phosphatase treatment of purified Nim1 and they were not detected in a strain that expressed a catalytically inactive form of Nim1 protein (Wu and Russell, 1993). Nim1 protein was present throughout the cell cycle, with no more than a twofold oscillation in abundance of Nim1 (Figure 2A). The relative abundance of the various mobility forms of Nim1 also did not appear to change dramatically during the cell cycle. Immunoblotting of extracts made from cells arrested in G_1, S, and G_2, using *cdc10-129*, hydroxyurea, and *cdc25-22* arrests, respectively, confirmed that Nim1 protein is present throughout these phases of the cell cycle (our unpublished data). Moreover, the electrophoretic mobility of Nim1 did not appear to undergo major changes at the cell cycle arrest points. These data indicate that neither the abundance nor the autophosphorylation activity of Nim1 vary greatly during the cell cycle.

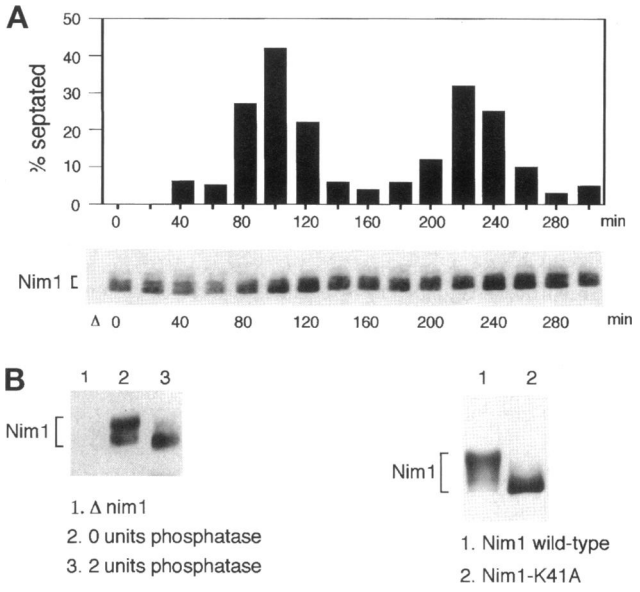

Figure 2. Nim1 protein abundance and autophosphorylation activity during the cell cycle. (A) Strain LW117, in which the genomic copy of *nim1*$^+$ encodes Nim1 protein having a C-terminal tag consisting of two copies of the HA epitope followed by six histidine residues was grown in rich YES medium to mid-log phase. Small cells in early G_2 were obtained by centrifugal elutriation and reinoculated into fresh media. Samples were collected every 20 min. Progression through two successive cycles was monitored by counting septating cells (top panel). Nim1 protein was purified from equal amounts of protein from cell extracts as described in MATERIALS AND METHODS. Immunoblotting was performed with anti-Nim1 antibody (bottom panel). Nim1 migrated as a series of bands in the ~70-kDa region of the gel. As expected, no signal was detected in samples prepared from a Δ*nim1* strain (lane 1 in immunoblot). The membrane was stained with Ponceau S to confirm that approximately equal amounts of a ~50-kDa protein that specifically binds to Ni^{2+}-NTA were present in each lane. (B) Nim1 protein isolated from *S. pombe* has reduced electrophoretic mobility due to phosphorylation. Anti-Nim1 antibody was used to precipitate Nim1-Ha6H from a Nim1 overproducer strain. The precipitated protein was treated with 2 U of potato acid phosphatase (lane 3) or buffer alone (lane 2) for 30 min at 30°C. Nim1 was detected by immunoblotting using monoclonal anti-HA (12CA5) antibody. Phosphatase treatment caused Nim1 to migrate with a faster electrophoretic mobility. Immunoprecipitation from a Δ*nim1* strain served as control (lane 1). (C) Inactive Nim1 migrates more rapidly in SDS-PAGE than active Nim1. Strains carrying plasmids that expressed Ha6H-tagged Nim1 (lane 1) or Nim1-K41A (lane 2) from the *nmt1*$^+$ promoter were grown in media lacking thiamine to induce Nim1 expression. Nim1 proteins were purified using Ni^{2+}-NTA and then analyzed by immunoblotting using anti-HA antibody.

Wee1 is a Nuclear Protein, whereas Nim1 is Predominantly Localized in the Cytoplasm

We next investigated the intracellular localization of Wee1 and Nim1 by use of immunofluorescence confocal microscopy. Since neither Wee1 nor Nim1 can be detected in wild-type cells, we first used a strain that expressed both the temperature-sensitive *wee1-50* allele and wild-type *nim1*$^+$ from the strong *adh1*$^+$ promoter. The strain was grown for several hours at 25°C before fixation to ensure that the Wee1 protein was in the active conformation. Affinity-purified anti-Wee1 antibodies produced a strong nuclear stain and a weak cytoplasmic signal (Figure 3). The same staining pattern was detected in cells that overproduced catalytically inactive Wee1 in a wild-type or Δ*nim1* background, indicating that Nim1 overproduction did not influence the localization of Wee1. Merging of the anti-Wee1 and propidium iodide DNA signals indicated that Wee1 was located both in the chromatin and nonchroma-

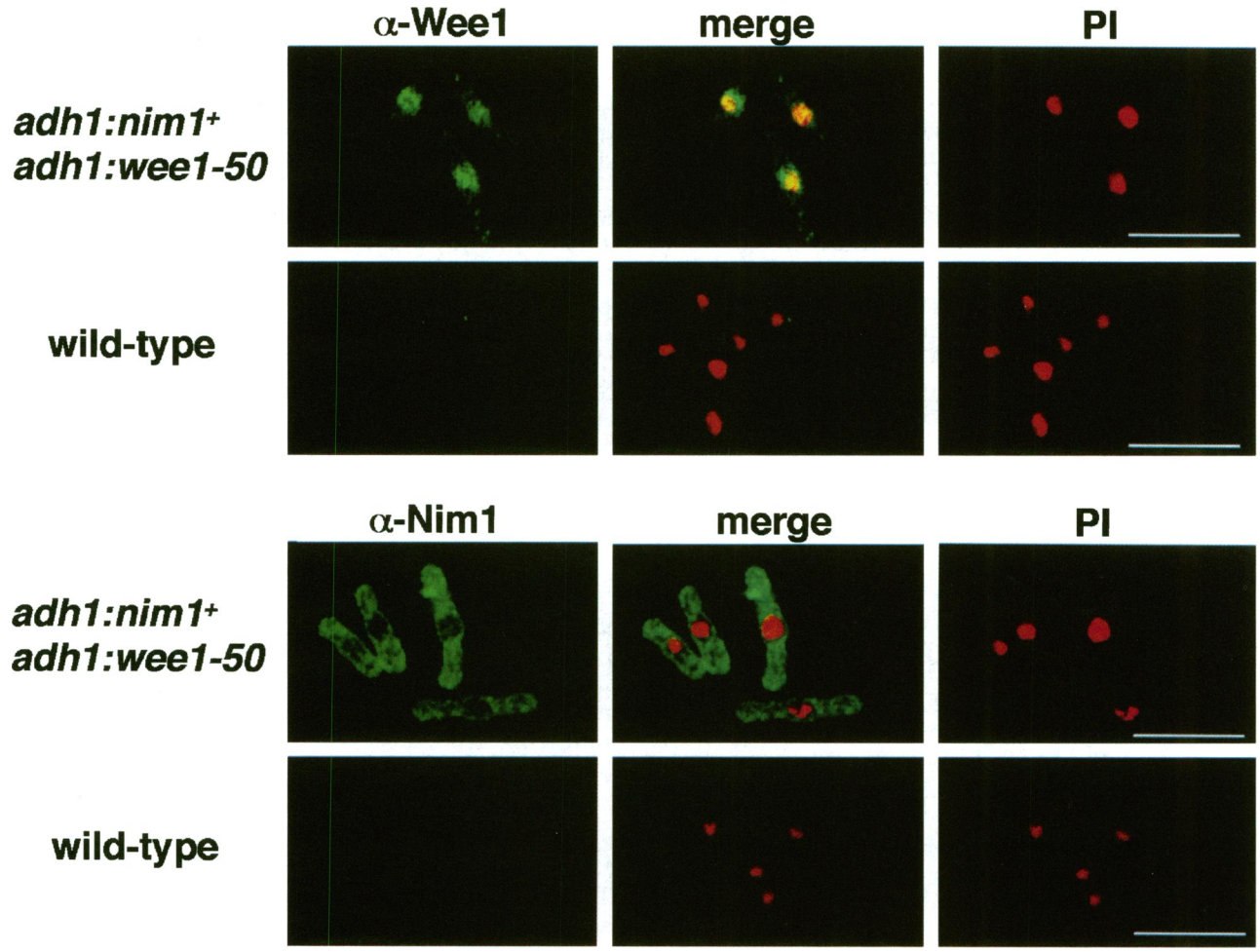

Figure 3. Wee1 is predominantly localized in the nucleus, whereas Nim1 is predominantly localized in the cytoplasm. Strain PR369 (*adh1:nim1*$^+$ *adh1:wee1-50*) was grown at 32°C to early log phase and shifted to 25°C for 4.5 h before fixation. Indirect confocal immunofluorescence was carried out using affinity-purified antibodies to Wee1 (top left panels) or Nim1 (bottom left panels) and FITC-conjugated secondary antibody. The nuclei were visualized by staining with PI (right panels). Merging of the green anti-Wee1 and red PI signals confirmed that Wee1 was predominantly nuclear, as indicated by the yellow signal in the top middle panels (merge). In contrast, there was essentially no overlap of the green anti-Nim1 and red propidium iodide signals, as indicated by the absence of yellow signal in the lower middle panels. Bar, 10 μm.

tin domains of the nucleus (Figure 3). Previous immunofluorescence light microscopy and immunogold electron microscopy studies demonstrated that the Cdc2-Cdc13 complex is located both in the nucleolar and chromatin domains of the nucleus during interphase (Booher *et al.*, 1989; Alfa *et al.*, 1990; Gallagher *et al.*, 1993), thus our findings show that Wee1 colocalizes with its substrate.

Genetic and biochemical studies have shown that Nim1 induces mitosis by directly phosphorylating and inactivating Wee1; therefore, we expected that Nim1 would be predominantly colocalized with Wee1 in the nucleus. In contravention of this prediction, affinity-purified anti-Nim1 antibodies stained the cytoplasm (Figure 3). Merging of the anti-Nim1 and DNA signals confirmed that there is very little or no Nim1 in the nucleus.

Nim1 Localization in Strains that Moderately Overproduce Nim1

The immunofluorescence confocal microscopy findings showing that Wee1 and Nim1 occupy different intracellular compartments were unexpected, because genetic and biochemical studies have established that Nim1 inhibits Wee1 via direct phosphorylation. A caveat to these immunolocalization findings was that they used strains that overproduced Nim1 and Wee1; therefore, it could be proposed that the anti-Nim1 or anti-Wee1 staining pat-

terns may not accurately represent the situation in wild-type cells. The Wee1 nuclear staining pattern appears reasonable because it assigns Wee1 to the same cellular compartment as Cdc2-Cdc13. To more carefully assess Nim1 localization, we performed two experiments to detect Nim1 in situations that more closely resemble the circumstances in wild-type cells. In the first experiment, we used a strain in which expression of *nim1*$^+$ was regulated by the thiamine-repressible *nmt1* promoter (Maundrell, 1993). The *nmt1:nim1*$^+$ construct was carried on an autonomously replicating plasmid, pREP1-Nim1. A culture of cells was grown to mid-log phase in medium containing thiamine, the cells were then washed and resuspended in thiamine-free medium. Cells were harvested for immunoblotting, immunolocalization, and cell size measurements at time points corresponding to 12 through 19 h after resuspension in thiamine-free medium. By immunoblotting with affinity-purified anti-Nim1 antibody, the Nim1 signal became readily detectable by 16.5 h and reached a maximum level at ~18 h (Figure 4A). A very long exposure of the immunoblot indicated that an increased Nim1 signal first became apparent at ~15 h. This time course of induction of the *nmt1* promoter closely corresponds to previous studies (Maundrell, 1990; Maundrell, 1993). Measurements of the length of dividing cells indicated that Nim1 overproduction first caused a measurable reduction in cell size at 14 to 15 h (Figure 4B). The cell size at division continued to decrease for the time course of the experiment, approaching a typical wee phenotype at 19 h.

We performed confocal immunofluorescence microscopy analysis of the samples from 12 through 19 h after resuspension in thiamine-free medium. A Nim1 signal first became weakly apparent at the 14-h time point and was readily detected at the 15-h time point (Figure 4C). At 14 h only a subset (~5%) of the cells had a Nim1 signal; this variability is presumably due to differences in plasmid copy number among cells in the population. At this early time point, the Nim1 signal was distinctly cytoplasmic, in fact there appeared to be little or no overlap of the Nim1 and DNA (propidium iodide, PI) signals (Figure 4C). At 15-h after resuspension in thiamine-free medium, the majority of the cells exhibited a Nim1 signal that was readily detected. As with the earlier time point, the Nim1 signal in cells from the 15-h sample was predominantly and perhaps exclusively cytoplasmic (Figure 4C). It is also evident from the data in Figure 4 that cells in the early stages of Nim1 overproduction were not wee, indicating that in terms of the ability of Nim1 to inhibit Wee1 and advance mitosis, the abundance of Nim1 was not saturating at the 14- and 15-h time points.

In the second experiment to assess Nim1 localization in cells that moderately overproduce Nim1, we examined a strain (LW449) having multiple integrated copies of a plasmid containing *nim1*$^+$. Immunoblot analysis using affinity-purified anti-Nim1 antibody indicated that Nim1 protein abundance was elevated ~5-fold in LW449 relative to the wild type (Figure 5A). LW449 underwent division at a cell length of 12.5 ± 0.3 μm (Table 2), a size that is intermediate between the wild-type (15.5 ± 0.8 μm) and the wee phenotype (division at ~8 μm) exhibited by *wee1*$^-$ cells or cells that highly overproduce Nim1 (Nurse, 1975; Russell and Nurse, 1987a). In LW449 cells, the anti-Nim1 signal was again predominantly detected in the cytoplasm (Figure 5B). Merging of the green anti-Nim1 signal and the red DNA propidium iodide signal indicated only very limited regions of the yellow colocalization signal, confirming that Nim1 was largely cytoplasmic in LW449 cells (Figure 5B). The fact that LW449 cells have a only semi-wee phenotype, as opposed to the typical wee phenotype of cells that grossly oveproduce Nim1, demonstrates that the Nim1 mitotic induction activity is not saturating in LW449 cells. Therefore, the predominantly cytoplasmic staining of Nim1 in LW449 cells is very likely to reflect the true subcellular localization of Nim1 protein in wild-type cells.

Diversion of Nim1 to the Nucleus Advances Mitosis

Taken at face value, the immunolocalization findings suggest that Nim1 may normally have limited access to Wee1 in vivo. A prediction which follows from this finding is that the timing of mitosis should be advanced if Nim1 is diverted into the nucleus, thus allowing greater access to Wee1. Targeting Nim1 to the nucleus was accomplished by attaching the SV40 large T antigen nuclear localization signal (NLS) to the C terminus of Nim1. The SV40 NLS consists of a highly basic polypeptide (PKKKRKV) that is capable of targeting non-nuclear proteins to nucleus (Kalderon *et al.*, 1984). A mutation (NLS*) changing the second lysine residue to asparagine (PKNKRKV) abolishes the nuclear-targeting activity of the polypeptide (Adam *et al.*, 1989). In the first part of the experiment, strains overproducing nim1-NLS and nim1-NLS* gene constructs from the *S. pombe nmt1* promoter were used for immunolocalization studies (Figure 6). These studies were carried out using a *cdc2-33* strain that was shifted to the restrictive temperature for 4 h, producing elongated cells in which the nuclear and cytoplasmic compartments could be more easily distinguished. This analysis showed that Nim1-NLS was very efficiently targeted to the nucleus (Figure 6, middle row), whereas Nim1-NLS* was excluded from the nucleus (Figure 6, top row). The same findings were

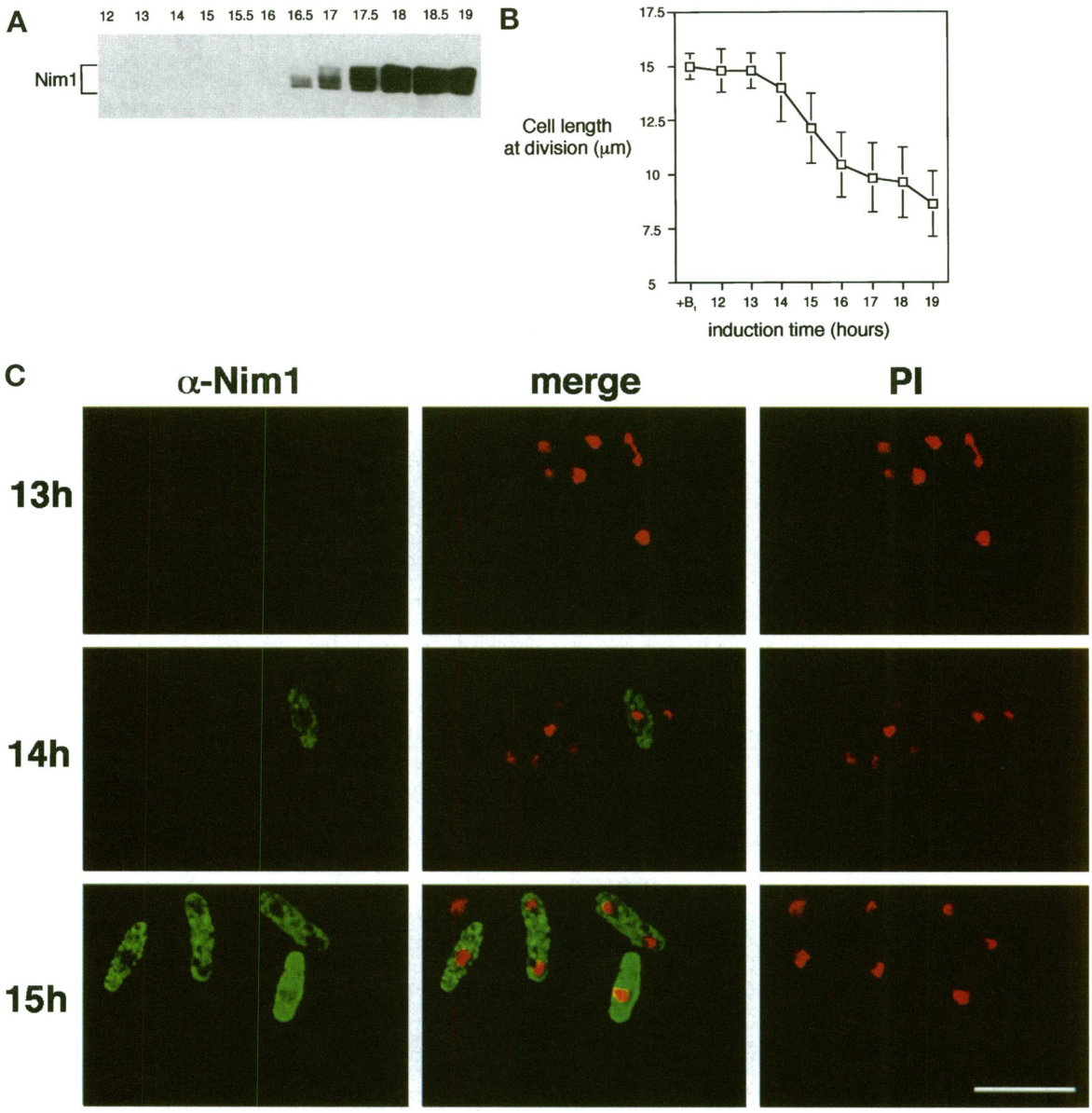

Figure 4. Nim1 is localized in the cytoplasm during the early phase of induced expression of *nmt1:nim1*$^+$. A wild-type strain (PR109) transformed with pREP1-Nim1 was grown to log phase in EMM2 medium containing thiamine and then washed and resuspended in thiamine-free medium. Cells were harvested for immunoblotting, immunolocalization, and cell size measurements at time points corresponding to 12 through 19 h after resuspension in thiamine-free medium. (A) Anti-Nim1 immunoblot showing the time course of the appearance of Nim1 protein. A very long exposure of the immunoblot indicated that an increased Nim1 signal first became apparent at ~15 h. (B) Cell length measurements of dividing cells during the time course. (C) Confocal immunofluorescence microscopy indicated that Nim1 protein is localized in the cytoplasm at 14 and 15 h after resuspension in thiamine-free medium (left panels). The nuclei were visualized by staining with PI (right panels); a merge of the anti-Nim1 and PI signals is shown in the middle panels. Nim1 protein was first detected at 14 h. The anti-Nim1 signal became progressively more intense at later times in a manner consistent with the immunoblot results shown in A. Bar, 10 μm.

obtained with cells grown at the permissive temperature.

Having established that Nim1 can be diverted to the nucleus by attachment of an active NLS, we next used gene conversion to replace genomic *nim1*$^+$ with *nim1*$^+$*-NLS* or *nim1*$^+$*-NLS**. This allowed us to examine the phenotypes caused by these constructs when they were expressed at wild-type levels from the *nim1*$^+$ promoter. The phenotypes of the *nim1*$^+$ and *nim1*$^+$*-NLS** strains were indistinguishable,

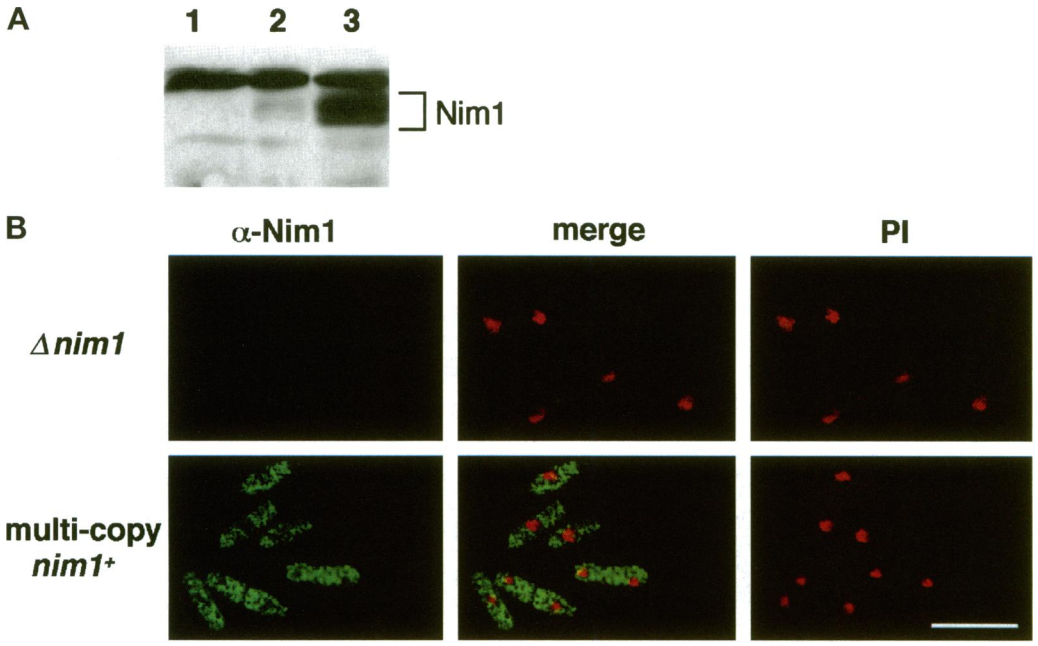

Figure 5. (A) Nim1 is found in the cytoplasm in a strain that contains multiple copies of *nim1*$^+$. (A) Cell extracts from Δ*nim1* (LW388), wild type (PR109), and a strain that contains multiple-integrated copies of *nim1*$^+$ cells (LW449) were analyzed by immunoblotting with affinity-purified anti-Nim1 antibody. A weak Nim1 signal is detected in wild-type cells that is absent in Δ*nim1* cells. In LW449 cells, the Nim1 signal is ~5-fold elevated relative to the wild type. A protein that is recognized by anti-Nim1 antibodies and migrates slightly slower than Nim1 serves as an internal control. (B) Confocal immunofluorescence microscopy studies performed with strains PR387 and LW449 using affinity-purified anti-Nim1 antibody. In LW449 cells, Nim1 was predominantly localized in the cytoplasm (bottom panels). No Nim1 signal was detected in the Δ*nim1* cells (PR387, top panels).

with cells dividing at 15.5 ± 0.8 μm and 15.7 ± 0.8 μm, respectively (Table 2). Thus, attachment of the mutant NLS had no effect on the mitotic induction activity of *Nim1*. In contrast, the *nim1*$^+$-NLS strain divided at 12.6 ± 1.0 μm, a ~20% size reduction relative to wild-type (Table 2). Thus, mitosis was

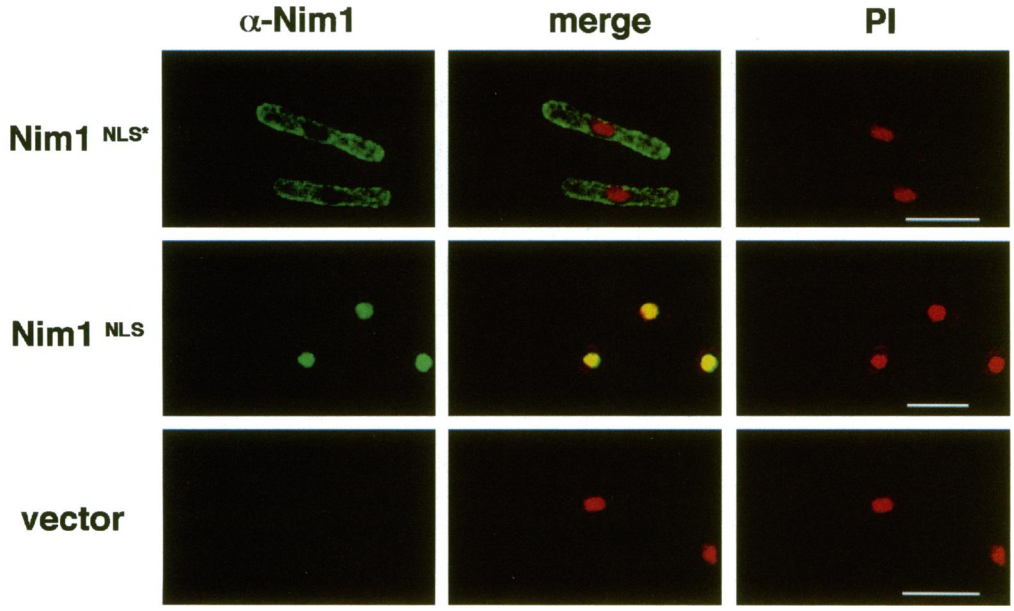

Figure 6. Attachment of the SV40 nuclear localization sequence (NLS) targets Nim1 to the nucleus. The SV40 NLS (PKKKRKV) or a mutant NLS (NLS*) sequence (PKNKRKV) was inserted at the 3′ end of *nim1*$^+$ and cloned into the *S. pombe* expression vector pREP1. Plasmids were transformed into a cdc2-33 strain (PR181). Cells were grown at 25°C in EMM2 without thiamine for 24 h to induce Nim1 expression. The cultures were incubated at 35.5°C for 4 h before fixation. Cells were stained with affinity-purified anti-Nim1 antibodies followed by FITC-conjugated secondary antibody (left panels). The nuclei were visualized by staining with propidium iodide (right panels). Signals were visualized by indirect confocal immunofluorescence. The anti-Nim1 and propidium iodide signals are merged in the middle panels. Nim1^{NLS*} appeared to be localized exclusively in the cytoplasm (top row), whereas Nim1^{NLS} appeared to be localized exclusively in the nucleus (middle row). No anti-Nim1 signal was detected in cells that did not overexpress Nim1 (lower row). Very similar staining patterns were detected in cells incubated at 25°C for 4 h before fixation. Bar, 10 μm.

Table 2. Division length of various strains

Strain	Genotype	Cell length at division
PR109	*nim1*$^+$	15.5 ± 0.8μm
LW424	*nim1-nls*	12.6 ± 1.0μm
LW425	*nim1-nls**	15.7 ± 0.8μm
LW449	*nim1*$^+$-multiple integrant	12.5 ± 0.3μm

Targeting Nim1 to the nucleus by expressing *nim1-nls* (LW424) causes cells to undergo cell division at reduced cell length, indicating an advancement of mitosis. A similar phenotype is observed in LW449 cells that overproduce Nim1 approximately fivefold above the wild-type level. Expression of Nim1 containing an inactive version of the SV40 NLS (*nim1-nls**) (LW425 cells) does not alter cell size.

advanced by targeting Nim1 to the nucleus. The cell size of the *nim1*$^+$-NLS strain was very similar to that of LW449 cells, which are estimated to have an ~5-fold increase in abundance of Nim1 protein (Table 2). This finding supports the conclusion that *Nim1* has restricted access to Wee1 protein in vivo.

DISCUSSION

Fission yeast has an accurate mechanism of linking the onset of mitosis with growth to a particular cell size, as demonstrated by the fact that in steady-state conditions there is very little variation in the cell size at which *S. pombe* cells initiate mitosis and undergo cell division (Mitchison, 1970). Genetic and biochemical studies have identified several key components of this mechanism, including Wee1 tyrosine kinase and Nim1 serine/threonine kinase. Wee1 inhibits the onset of mitosis by carrying out the inhibitory tyrosyl phosphorylation of Cdc2-Cdc13, whereas Nim1 promotes the onset of mitosis by carrying out inhibitory phosphorylation of Wee1. It is not known how the Nim1-Wee1-Cdc2 kinase cascade is used to monitor cell size. It is supposed that the cell size monitoring mechanism involves some type of communication between the nucleus and cytoplasm, in part because there is a direct correlation between ploidy and cell size at mitosis.

In this report, we have provided evidence that the Nim1-Wee1-Cdc2 kinase cascade proceeds from the cytoplasm to the nucleus. This conclusion is based both on immunofluorescence confocal microscopy and genetic data. Immunofluorescence confocal microscopy has shown that Nim1 is localized in the cytoplasm while Wee1 is predominantly localized in the nucleus. Wee1 and Nim1 proteins are expressed at very low levels in wild-type cells; therefore, the microscopy studies were necessarily carried out with Wee1 and Nim1 overproducer strains. As mentioned above, there appears to be little reason to doubt the validity of the data showing that Wee1 is predominantly found in the nucleus, even though these experiments used cells that highly overproduced Wee1. Cdc2-Cdc13 complex is localized in the nucleus (Booher *et al.*, 1989), thus our immunolocalization findings place Wee1 in the same cellular compartment as its key substrate. Moreover, nuclear localization of Wee1 is consistent with the localization of full-length human Wee1 protein to the nucleus in human cells (McGowan and Russell, 1995).

Localization of Nim1 to the cytoplasm is surprising because a combination of genetic and biochemical studies have established that Nim1 induces mitosis by directly phosphorylating Wee1 (Russell and Nurse, 1987a; Coleman *et al.*, 1993; Parker *et al.*, 1993; Wu and Russell, 1993). For this reason we have confirmed our immunolocalization findings with cells that only moderately overproduce Nim1. Nim1 is found in the nucleus in cells that are in the very early stages of induction of the *nmt1:nim1*$^+$ construct. In fact, in this experiment we were able to detect Nim1 in the cytoplasm before the point at which Nim1 becomes readily detectable by immunoblotting. Moreover, we have shown that Nim1 is cytoplasmic in cells that constantly overproduce Nim1 ~5-fold above the wild type. In these conditions, the abundance of Nim1 is clearly in the rate-limiting range, which strongly suggests that the localization pattern is reflective of the wild-type situation.

Where do Nim1 and Wee1 interact in vivo? There are two types of models that could explain how a protein that predominantly localizes to the cytoplasm can interact with a substrate that is predominantly found in the nucleus. The first model proposes that Nim1 phosphorylates newly synthesized Wee1 before the translocation of Wee1 from the cytoplasm to the nucleus. This model assumes that Wee1 is only slowly dephosphorylated after its translocation to the nucleus. The second model proposes that either Wee1 or Nim1 shuttle between the nucleus and the cytoplasm. Wee1 could shuttle into the cytoplasm and be phosphorylated by Nim1 or Nim1 could shuttle into the nucleus and phosphorylate Wee1. We have no reason to favor either possibility in the shuttling model, although we note that Wee1 activity is dependent on an interaction with Swo1, a Hsp90 protein in fission yeast (Aligue *et al.*, 1994). Hsp90 proteins have been implicated in the shuttling of steroid receptors between the nucleus and the cytoplasm (Bohen and Yamamoto, 1993). Whichever model is correct, an important aspect of our findings is that they provide evidence of a regulatory network, the Nim1-Wee1-Cdc2 cascade, that links the activity of nuclear Cdc2-Cdc13 with signals emanating from the cytoplasm. We propose that the cellular distribution of the Nim1-Wee1-Cdc2

cascade is important for coordinating the onset of mitosis with cellular growth.

ACKNOWLEDGMENTS

The assistance of George Klier and Kevin Sullivan was invaluable for confocal microscopy. Beth Furnari kindly provided the Northern blot. We also thank Clare McGowan and Janet Leatherwood for their helpful comments. This work was supported by fellowships from the Human Frontiers Science Program and the California Division of the American Cancer Society (K.S.), European Molecular Biology Organization and Minesterio de Educacion y Ciencia/Spain (R.A.), and a grant from the National Institutes of Health (P.R.).

REFERENCES

Adam, S.A., Lobl, T.J., Mitchell, M.A., and Gerace, L. (1989). Identification of specific binding proteins for a nuclear localization sequence. Nature *337*, 276–279.

Alfa, C.E., Ducommun, B., Beach, D., and Hyams, J.S. (1990). Distinct nuclear and spindle pole body population of cyclin-cdc2 in fission yeast. Nature *347*, 680–682.

Aligue, R., Akhavan-Niaki, H., and Russell, P. (1994). A role for Hsp90 in cell cycle control: Wee1 tyrosine kinase activity requires interaction with Hsp90. EMBO J. *13*, 6099–6106.

Barbet, N., Muriel, W.J., and Carr, A.M. (1992). Versatile shuttle vectors and genomic libraries for use with *Schizosaccharomyces pombe*. Gene *114*, 59–66.

Bohen, S.P., and Yamamoto, K.R. (1993). Isolation of Hsp90 mutants by screening for decreased steroid receptor function. Proc. Natl. Acad. Sci. USA *90*, 11424–11428.

Booher, R.N., Alfa, C.E., Hyams, J.S., and Beach, D.H. (1989). The fission yeast cdc2/cdc13/suc1 protein kinase: regulation of catalytic activity and nuclear localization. Cell *58*, 485–497.

Coleman, T.R., Tang, Z., and Dunphy, W.G. (1993). Negative regulation of the Wee1 protein kinase by direct action of the Nim1/Cdr1 mitotic inducer. Cell *72*, 919–929.

Dunphy, W.G. (1994). The decision to enter mitosis. Trends Cell Biol. *4*, 202–207.

Featherstone, C., and Russell, P. (1991). Fission yeast p107wee1 mitotic inhibitor is a tyrosine/serine kinase. Nature *349*, 808–811.

Feilotter, H., Nurse, P., and Young, P. (1991). Genetic and molecular analysis of the cdr1/nim1 in *Schizosaccharomyces pombe*. Genetics *127*, 309–318.

Gallagher, I.M., Alfa, C.E., and Hyams, J.S. (1993). $p63^{cdc13}$, a B-type cyclin, is associated with both the nucleolar and chromatin domains of the fission yeast nucleus. Mol. Biol. Cell *4*, 1087–1096.

Gould, K.L., Moreno, S., Owen, D.J., Sazer, S., and Nurse, P. (1991). Phosphorylation at Thr167 is required for *Schizosaccharomyces pombe* $p34^{cdc2}$ function. EMBO J. *10*, 3297–3309.

Gould, K.L., Moreno, S., Tonks, N.K., and Nurse, P. (1990). Complementation of the mitotic activator, $p80^{cdc25}$, by a human protein-tyrosine phosphatase. Science *250*, 1573–1576.

Gould, K.L., and Nurse, P. (1989). Tyrosine phosphorylation of the fission yeast $cdc2^{+}$ protein kinase regulates entry into mitosis. Nature *342*, 39–45.

Kalderon, D., Richardson, W.D., Markham, A.F., and Smith, A.E. (1984). Sequence requirements for nuclear location of simian virus 40 large-T antigen. Nature *311*, 33–38.

Kovelman, R., and Russell, P. (1996). Stockpiling of Cdc25 during a DNA replication checkpoint arrest in *Schizosaccharomyces pombe*. Mol. Cell. Biol *16*, 86–93.

Lee, M.S., Enoch, T., and Piwnica-Worms, H. (1994). mik1 encodes a tyrosine kinase that phosphorylates $p34^{cdc2}$ on tyrosine-15. J. Biol. Chem. *269*, 30530–30537.

Lowndes, N.F., McInerny, C.J., Johnson, A.L., Fantes, P.A., and Johnston, L.H. (1992). Control of DNA synthesis genes in fission yeast by the cell-cycle gene $cdc10^{+}$. Nature *355*, 449–453.

Lundgren, K., Walworth, N., Booher, R., Dembski, M., Kirschner, M., and Beach, D. (1991). mik1 and wee1 cooperate in the inhibitory tyrosine phosphorylation of cdc2. Cell *64*, 1111–1122.

Maundrell, K. (1990). nmt1 of fission yeast. J. Biol. Chem. *265*, 10857–10864.

Maundrell, K. (1993). Thiamine-repressible expression vectors pREP and pRIP for fission yeast. Gene *123*, 127–130.

McGowan, C.H., and Russell, P. (1993). Human Wee1 kinase inhibits cell division by phosphorylating $p34^{cdc2}$ exclusively on Tyr15. EMBO J. *12*, 75–85.

McGowan, C.H., and Russell, P. (1995). Cell cycle regulation of human WEE1. EMBO J. *14*, 2166–2175.

Millar, J.B.A., Lenaers, G., and Russell, P. (1992). Pyp3 PTPase acts as a mitotic inducer in fission yeast. EMBO J. *11*, 4933–4941.

Millar, J.B.A., McGowan, C.H., Lenaers, G., Jones, R., and Russell, P. (1991). $p80^{cdc25}$ mitotic inducer is the tyrosine phosphatase that activates G_2-phase p34cdc2 kinase in fission yeast. EMBO J. *10*, 4301–4309.

Mitchison, J.M. (1970). Physiological and cytological methods for *Schizosaccharomyces pombe*. Meth. Cell Physiol. *4*, 131–146.

Moreno, S., Hayles, J., and Nurse, P. (1989). Regulation of $p34^{cdc2}$ protein kinase during mitosis. Cell *58*, 361–372.

Moreno, S., Klar, A., and Nurse, P. (1991). Molecular genetic analysis of fission yeast *Schizosaccharomyces pombe*. Methods Enzymol. *194*, 795–823.

Nurse, P. (1975). Genetic control of cell size at cell division in fission yeast. Nature *256*, 547–551.

Parker, L.L., Atherton-Fessler, S., and Piwnica-Worms, H. (1992). $p107^{wee1}$ is a dual-specificity kinase that phosphorylates $p34^{cdc2}$ on tyrosine 15. Proc. Natl. Acad. Sci. USA *89*, 2917–2921.

Parker, L.L., Walter, S.A., Young, P.G., and Piwnica-Worms, H. (1993). Phosphorylation and inactivation of the mitotic inhibitor Wee1 by the nim1/cdr1 kinase. Nature *363*, 736–738.

Russell, P., and Nurse, P. (1986). $cdc25^{+}$ functions as an inducer in the mitotic control of fission yeast. Cell *45*, 145–153.

Russell, P., and Nurse, P. (1987a). The mitotic inducer $nim1^{+}$ functions in a regulatory network of protein kinase homologs controlling the initiation of mitosis. Cell *49*, 569–576.

Russell, P., and Nurse, P. (1987b). Negative regulation of mitosis by $wee1^{+}$, a gene encoding a protein kinase homolog. Cell *49*, 559–567.

Shiozaki, K., and Russell, P. (1995). Cell-cycle control linked to the extracellular environment by MAP kinase pathway in fission yeast. Nature *378*, 739–743.

Wu, L., and Russell, P. (1993). Nim1 kinase promotes mitosis by inactivating Wee1 tyrosine kinase. Nature *363*, 738–741.

Young, P.G., and Fantes, P.A. (1987). *Schizosaccharomyces* mutants affected in their division response to starvation. J. Cell Sci. *88*, 295–304.